

PACS numbers: 42.55.Rz; 42.60.Da; 42.60.Lh; 42.62.Fi
DOI: 10.1070/QE2012v042n12ABEH014972

Tunable repetitively pulsed Cr^{2+}:ZnSe laser

A.S. Egorov, O.N. Eremeykin, K.Yu. Pavlenko, A.P. Savikin, V.V. Sharkov

Abstract. **Methods of wavelength tuning of a polycrystalline Cr^{2+}:ZnSe laser pumped by a repetitively pulsed Tm:YLF laser (pulse duration ~100 ns, pulse repetition rate 3 KHz) are studied. With the use of a prism selector, the laser wavelength was tuned within the range of 2070–2400 nm at a linewidth of 11 nm for a SiO_2 prism and 30 nm for a CaF_2 prism. The use of a Lyot filter made it possible to tune the Cr^{2+}:ZnSe laser wavelength (with replacement of the cavity mirrors) within the spectral ranges of 2130–2400 and 2530–2750 nm at a linewidth of 4 nm.**

Keywords: *mid-IR region, Tm:YLF laser, polycrystalline Cr^{2+}:ZnSe laser, prism selector, Lyot filter.*

1. Introduction

Tunable mid-IR lasers are of interest for detecting molecular gases with low concentrations, which is an important problem of environmental monitoring, as well as for various medical, chemical, and industrial applications [1].

These needs can be partially satisfied by using tunable crystalline Cr^{2+}:ZnSe lasers emitting in the wavelength region 2–3 μm, which includes intense absorption lines of most simple molecules [2–6].

Wavelength tuning of lasers with a dispersive cavity is mainly performed using a prism [7–13], an interference-polarisation filter (IPF) (Lyot filter) [14, 15], or a diffraction grating [16–18]. In particular, the use of a ZnSe prism in a Cr^{2+}:ZnSe laser pumped by a cw Tm:YAP laser allowed the authors of [7] to obtain tuning within the range 2138–2760 nm with the linewidth of ~30 nm in the centre and ~10 nm at the edges of the tuning range. Introduction of an additional etalon inside the cavity decreases the linewidth to 4 nm.

By placing a fused-quartz prism or a quartz birefringent filter 0.8 mm thick in the cavity of a cw Cr^{2+}:ZnSe laser, the authors of [14] managed to obtain the linewidth narrower than 0.4 nm within the tuning range 2180–2800 nm.

In the pulsed regime (pulse duration 10 ms), tuning within the range 2246–2650 nm was achieved using a quartz plate 1.5 mm thick oriented at the Brewster angle [15].

A.S. Egorov, K.Yu. Pavlenko, A.P. Savikin, V.V. Sharkov
N.I. Lobachevsky Nizhnii Novgorod State University, prosp. Gagarina 23, 603950 Nizhnii Novgorod, Russia; e-mail: aegorovnn@yandex.ru;
O.N. Eremeykin G.G. Devyatykh Institute of Chemistry of High-Purity Substances, Russian Academy of Sciences, ul. Tropinina 49, 603950 Nizhnii Novgorod, Russia

Received 10 September 2012; revision received 25 October 2012
Kvantovaya Elektronika **42** (12) 1106–1110 (2012)
Translated by M.N. Basieva

Using a 600-line mm^{-1} diffraction grating as a selector, laser wavelength in [16] was tuned from 2120 to 2770 nm at a linewidth smaller than 2 nm. The use of crystals with a low concentration of Cr^{2+} ions and a sapphire prism allowed one to obtain wavelength tuning within the range 1880–3100 nm in the repetitively pulsed regime [10].

The widest tuning range (1973–3349 nm) was achieved for a ceramic Cr^{2+}:ZnSe laser with a dispersive cavity and a CaF_2 prism under pumping by an Er^{3+} fibre laser (wavelength $\lambda = 1697$ nm) [13].

Nevertheless, available papers provide no sufficient information for determining the dispersive cavity parameters that allow one to obtain lasing with required spectral characteristics. The aim of the present work is to study and compare two methods of tuning the radiation of a repetitively pulsed Cr^{2+}:ZnSe laser, namely, tuning by a dispersive prism and by a Lyot filter. For the studied selectors, we present the experimental results and the theoretical estimates of the main parameters, such as tuning range, angular tuning rate, lasing linewidth, free dispersion region, sharpness factor, etc. The nonselective losses introduced by these elements are also presented.

2. Prism selector

Selection in a dispersive cavity with a prism occurs due to deflection of laser beams with different wavelengths at different angles to the cavity axis. The selective losses in this case depend on the cavity alignment. The longitudinal modes propagating orthogonally to the reflecting surfaces of mirrors have the lowest losses.

The selective characteristics of a cavity with a prism are determined by its angular dispersion $d\varphi/d\lambda$. If the prism faces are oriented at the Brewster angle α_{Br} to the optical axis of the cavity, the expression for the angular dispersion has the form $d\varphi/d\lambda = 2dn/d\lambda$ (n is the refractive index) [19]. The angular tuning rate K of a prism cavity is inversely proportional to the prism material dispersion,

$$K = (2dn/d\lambda)^{-1}. \quad (1)$$

For the prism resolution $R \approx \lambda/\delta\lambda$ determined by the instrumental diffraction profile [19], the cavity transmission linewidth $\delta\lambda_{tr}$ can be found as

$$\delta\lambda_{tr} = \frac{\lambda}{2w}\left(\frac{dn}{d\lambda}\right)^{-1}\frac{\cos\alpha_{Br}\cos(A/2)}{2\sin A}, \quad (2)$$

where w is the beam radius. The refracting angle of the prism whose faces are oriented at the Brewster angle to the cavity optical axis is determined by the expression [19]

$$A = 2\arcsin[(n^2 + 1)^{-1/2}]. \quad (3)$$

As follows from relations (1) and (2), the prisms made of a material with a high dispersion provide better spectral selectivity (Table 1).

Table 1. Comparison of the selective properties of SiO_2 and CaF_2 prisms (experimental values are given in parentheses).

Prism material	λ/μm	n	$\frac{dn}{d\lambda}$/μm^{-1}	A/deg	K/ nm ang.min^{-1}	$\delta\lambda_{tr}$/ nm
SiO_2 (fused quartz)	2.2	1.43501	–0.0161	69.7	9 (9)	22
CaF_2	2.2	1.42281	–0.00541	70.2	26.9 (23)	65

We experimentally studied the lasing characteristics of a Cr^{2+}:ZnSe laser with a dispersive cavity (Fig. 1). The Cr^{2+}:ZnSe active element (Cr^{2+} concentration $\sim 10^{18}$ cm^{-3}) had the form of a disk 4 mm thick with a diameter of 20 mm and two polished faces. To reduce the undesirable selection of the laser spectrum caused by interference effects, the active element was positioned at the Brewster angle with respect to the optical axis of the cavity.

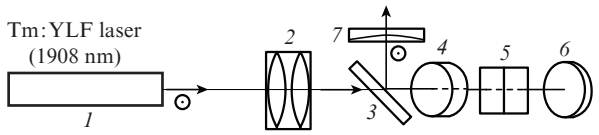

Figure 1. Scheme of a Cr^{2+}:ZnSe laser with a prism selector: (*1*) Tm:YLF laser; (*2*) lens system; (*3*) dichroic mirror; (*4*) Cr^{2+}:ZnSe active element; (*5*) prism selector; (*6*) highly reflecting mirror; (*7*) output mirror.

The Cr^{2+}:ZnSe polycrystal was excited by the linearly polarised radiation of a diode-pumped Tm:YLF laser with $\lambda_{pump} = 1908$ nm. So that the beams reflected from the optical units of the Cr^{2+}:ZnSe laser cavity did not hit the pump laser, the optical cavity axis was inclined at 1.5° with respect to the pump beam direction. The pump pulse duration was $\Delta t_{pump} \approx$ 100 ns at the pulse repetition rate $f_{rep} = 3$ kHz.

A beam of the Tm:YLF laser (*1*) was focused by a lens system (*2*) inside the Cr^{2+}:ZnSe sample (*4*). The cavity 100 mm long was formed by mirrors (*3*), (*5*), and (*7*). The plane mirror (*6*) had a high reflection coefficient at wavelengths of 1.9–2.4 μm (no lower than 99.5%), while the dichroic mirror (*3*) had a high reflection coefficient within the range 2.1–2.4 μm (~99% for the vertical polarisation) and a high transmission coefficient at the pump wavelength (~90%). As an output mirror, we used the spherical mirror (*7*) with a curvature radius of 300 mm and a refection coefficient of 78% at the laser wavelength. The pulse duration of the Cr^{2+}:ZnSe laser was$\Delta t_{gen} \approx 70$ ns. The dispersive prism (*5*) was placed between the active medium and highly reflecting mirror (*6*). The output laser radiation was tuned by changing the angle of rotation of the highly reflecting mirror. The power was measured by a calibrated Gentec detector with the spectral sensitivity region 0.5–10 μm. The temporal parameters of the laser radiation were measured by a photodetector based on a KPT-structure with a time constant of $\sim 5 \times 10^{-9}$ s. Spectral analysis of the output radiation in the range 2.1–2.8 μm was performed using a Solar M833 diffraction monochromator. A computer system based on a National Instruments NI PCI 6251 card was used for remote control of the monochromator motor and for data accumulation and processing. The control, data processing, and graphic display software was developed in the LabVIEW programming environment.

The effect of the material dispersion on the spectral characteristics of laser radiation was studied using prisms made of fused quartz SiO_2 ($dn/d\lambda = -0.0161$ μm^{-1}) and CaF_2 ($dn/d\lambda = -0.00541$ μm^{-1}). The SiO_2 prism [Fig. 2, curve (*1*)], as well as the CaF_2 prism [Fig. 2, curve (*2*)], allowed us to tune the output radiation wavelength in the spectral range $\Delta\lambda$ = 2070–2400 nm. The long-wavelength limit of the tuning range was determined by the spectral dependence of the reflection coefficients of the cavity mirrors (Fig. 2). The short-wavelength edge was determined by the active medium absorption [1]. The dip in the tuning curve is related to the absorption of laser radiation by the quartz prism material.

In the dispersive cavity with a fused quartz prism, the FWHM of the spectral line with $\lambda = 2200$ nm [Fig. 3, curve (*1*)] was 11 nm and decreased to 5–7 nm at the tuning curve edges. This narrowing of the spectrum can be explained by

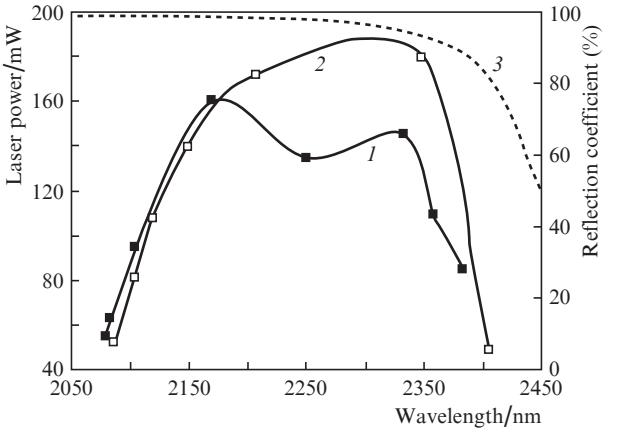

Figure 2. Tuning curves of the Cr^{2+}:ZnSe laser with a SiO_2 (*1*) and CaF_2 (*2*) prism at a pump power of 800 mW, as well as wavelength dependence of the reflection coefficient of the highly reflecting mirror of the Cr^{2+}:ZnSe laser cavity (*3*).

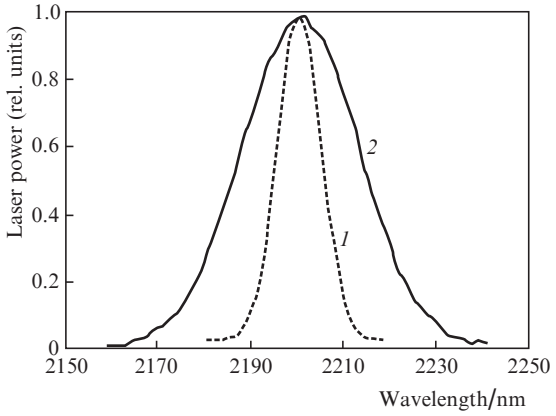

Figure 3. Spectra of a Cr^{2+}:ZnSe laser with a selective cavity and a SiO_2 (*1*) or CaF_2 (*2*) prisms.

the near-threshold lasing regime at the tuning range edges. The angular tuning rate was $K = 9$ nm ang.min^{-1}.

With the CaF_2 prism selector, the laser linewidth at a wavelength of 2200 nm was $\delta\lambda \approx 30$ nm [Fig. 3, curve (*2*)] at a pump power exceeding the threshold value by a factor of 2.5. Similar to the case with the SiO_2 prism, the laser line became narrower (to 13–15 nm) at the tuning edges. The tuning rate for the cavity with the CaF_2 prism was $K =$ 23 nm ang.min^{-1}.

The introduction of prisms lead to a slight increase in the lasing threshold and to a decrease in the output power by ~23% for the SiO_2 prism and by ~7% for the CaF_2 prism when the cavity was adjusted to the maximum gain. The nonselective losses introduced by the prisms can be related to the absorption by the material and by the reflection of the nonlinearly polarised beam from the prism faces. The polarisation ellipticity can be caused by both the natural and thermally induced anisotropy of the active medium. In addition, the losses can be caused by the Fresnel reflection form the faces of the prism with the refracting angle A different from the optimal value calculated by expression (3).

3. Selective cavity with a Lyot filter

Compared to other dispersive elements, an IPF (or Lyot filter), as well as a prism with faces oriented at the Brewster angle, has the minimal nonselective losses [20]. Similar to the case with prisms, the absence of dielectric coating ensures a low sensitivity of the filter to the radiation power density, which is determined only by the radiation resistance of the material. The sensitivity of IPFs to laser radiation divergence is also low, because of which it is not necessary to use an intracavity collimating optical system.

In experiment, we placed a two-stage Lyot filter into the Cr^{2+}:ZnSe laser between the dichroic mirror (*3*) and the output mirror (*6*) (Fig. 4). The mirror (*3*) simultaneously served as a linear polariser at the laser wavelength. The Lyot filter was formed by a pair of birefringent plane-parallel plates with the thicknesses $d_1 = 2$ mm and $d_2 = 6$ mm, which were cut from crystalline quartz parallel to the optical axis. The plates were mounted in a holder fixed on a rotary table with a step motor (Standa), which ensured the rotation angle accuracy of 0.9′. The laser frequency was tuned by rotating the holder with the plates around the normal to their faces. The rotary table with the IPF and the monochromator were controlled by a National Instruments computer system.

The faces of the plates were oriented at the Brewster angle α_{Br} to the cavity axis and served as partial polarisers. A wave polarised in the plane of incidence (p-polarisation) passed through the surfaces of the plates without losses. A wave with the orthogonal polarisation (s-polarisation) was partially attenuated. In this case, the transmission of the faces for the s-polarisation is given by the expression

$$\tau_s = \frac{2n}{n^2 + 1},$$

where $n = (n_o + n_e)/2$, and n_o and n_e are the refractive indices for the ordinary and extraordinary waves, respectively [21]. At the wavelength $\lambda \approx 2.3$ μm, the transmission is $\tau_s \approx 92\%$.

The filter transmission is a periodic function of wavelength and depends on the angle of incidence α on the plate and on the angle Φ between the main plane of the birefringent plate and the plane of beam incidence on the front face [19],

$$T = \cos^2\Delta\varphi(\alpha, \Phi), \tag{4}$$

where $\Delta\varphi$ is the difference between the phase incursions for the ordinary and extraordinary waves. The laser frequency can be tuned by changing the angle of inclination of the anisotropic plates of the filter, i.e., by changing the angle α. At the normal incidence of a light wave on the plate surface ($\alpha = 90°$), the dependence of the transmission coefficient on the wavelength is described by the expression

$$T = \cos^2\left[\frac{\pi(n_e - n_o)\,d}{\lambda}\right], \tag{5}$$

where d is the filter thickness.

As the angle α deviates from α_{Br}, the nonselective losses for the p-polarisation increase. Therefore, tuning is usually performed by rotating the plates around the normal to the front face, i.e., by changing the angle Φ [22, 23].

With rotation of the plate around the normal, the distances l_o and l_e passed by the o- and e-beams remain constant. The refractive index n_e for the extraordinary beam changes due to the change in the angle θ between the wave vector $\boldsymbol{k}$ and the optical axis of the anisotropic plate. In this case, one uses the following angular dependence of the extraordinary refractive index [24]:

$$n^e(\theta) = n_o\sqrt{\frac{1 + \tan^2\theta}{1 + (n_o/n_e)^2\tan^2\theta}}. \tag{6}$$

The angle θ is determined according to the expression

$$\theta = \arccos\left(\frac{\sin\alpha}{n_o}\cos\Phi\right). \tag{7}$$

When deriving this expression, we assumed that $l_o \approx l_e$, because the overlap of the o- and e-beams remained the same after passing through the plate.

When the plane of incidence is perpendicular to the main plane ($\Phi = 90°$), the extraordinary refractive index does not depend on the angle α and takes an extremal value. In this case, the difference in the refractive indices is maximum and the free dispersion region $\Delta\lambda$ of the filter is minimal. When the plane of incidence coincides with the main plane ($\cos\Phi = 1$), the refractive index n^e is different in different directions. The region $\Delta\lambda$ was estimated using the following expression taking into account the different orientations of the anisotropic plate with respect to the incident beam:

$$\Delta\lambda = \frac{\lambda^2}{[n^e(\theta) - n_o]d[1 - (\sin^2\alpha_{Br})/n_o^2]^{-1/2}}. \tag{8}$$

The dependence of $\Delta\lambda$ on the angle Φ was theoretically and experimentally studied for a plate with the thickness $d_2 =$

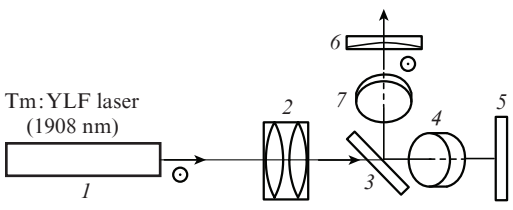

Figure 4. Scheme of a Cr^{2+}:ZnSe laser with a Lyot filter: (*1*) Tm:YLF laser; (*2*) lens system; (*3*) dichroic mirror; (*4*) Cr^{2+}:ZnSe active element; (*5*) highly reflecting mirror; (*6*) output mirror; (*7*) Lyot filter.

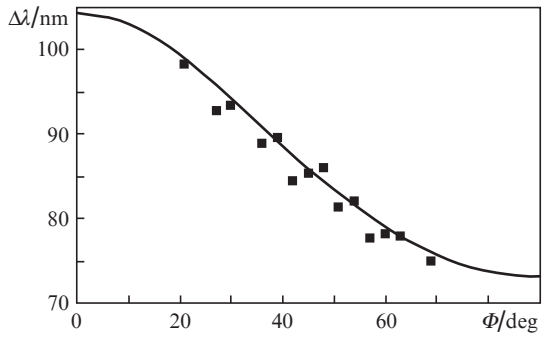

Figure 5. Theoretical (curve) and experimental (points) dependences of the free dispersion region $\Delta\lambda$ on the angle Φ.

6 mm (Fig. 5). The distance $\Delta\lambda_1$ between the transmission maxima of the filter used in the experiment was determined by the thinner plate with the thickness d_1. At $\Phi = 45°$, according to (7) and (8), $\Delta\lambda_1 \approx 260$ nm, which approximately corresponded to the laser tuning range.

The laser wavelength was tuned within a range of 2130–2400 nm (Fig. 6). Similar to the case with the prism, the long-wavelength edge of the tuning range was determined by the spectral dependence of the reflection coefficients of the cavity mirrors. In the short-wavelength region, the tuning range was limited by the filter design.

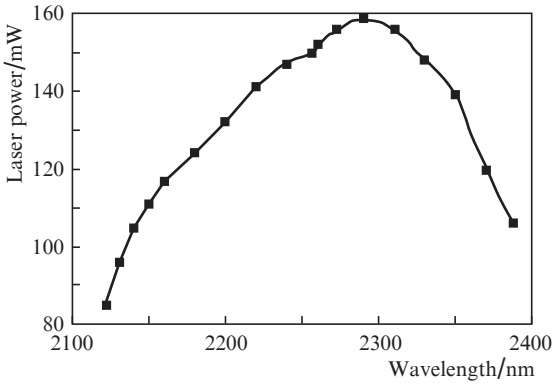

Figure 6. Tuning curve of the Cr^{2+}:ZnSe laser with a Lyot filter at a pump power of 800 mW.

The tuning rate was 8.5 nm deg^{-1}. In the course of experiment, it was found that the use of the two inner surfaces of the birefringent plates, which served as partial polarizers, is insufficient for polarisation isolation of the filter plates since the lasing spectrum contained, in addition to the main maximum, additional (spurious) maxima with a lower intensity. To eliminate the spurious maxima, it was necessary to introduce an additional pair of fused quartz plates between the birefringent plates.

The spectral FWHM of the laser line did not exceed $\delta\lambda \sim 4$ nm at $\lambda \approx 2300$ nm (Fig. 7). From the experiment with the plate with the thickness $d_2 = 6$ mm, we determined the sharpness factor $F = \Delta\lambda/\delta\lambda$, which characterises the selective property of the Lyot filter, to be ~25.

It may be of interest to use a selective cavity simultaneously with a prism and a single-plate Lyot filter. In particular, taking into account the fond F, the combination of a quartz

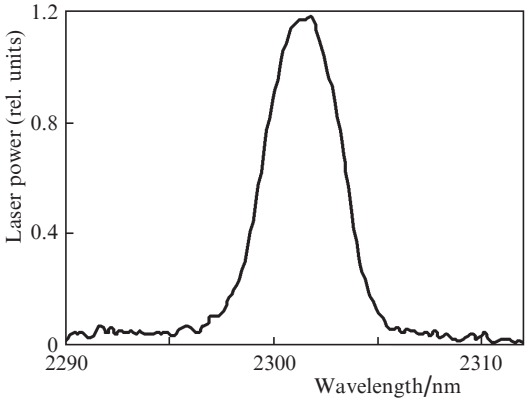

Figure 7. Spectrum of the Cr^{2+}:ZnSe laser with a Lyot filter.

prism and a birefringent quartz plate ~25 mm thick will allow one to decrease the laser linewidth to $\delta\lambda < 1$ nm. Due to birefringence, an increase in the anisotropic plate thickness will cause a shift of the e-beam with respect to the o-beam by the value

$$h \approx d\tan\beta, \tag{9}$$

where

$$\beta(\theta) = -\arctan\left[\left(\frac{n_o}{n_e}\right)^2 \tan\theta\right] + \theta \tag{10}$$

is the birefringence angle between the normal to the tangent to the ellipsoid of revolution and the wave vector, which depends on the angle θ [23]. According to (9) and (10), for the angle $\theta = 45°$, the beams at the distance $d = 25$ mm are separated by $h \approx 0.13$ mm. Taking into account that the diameter of the excited cavity mode is ~1 mm, the shift should exert no negative effect on the selective properties of the Lyot filter.

The nonselective losses introduced by the IPF were insignificant and lead to a decrease in the laser output power by about 4%. This was probably related to absorption losses in the optical components of the filter. At the pump power of 6 W, the laser output power at a wavelength of 2300 nm was ~2 W, which is somewhat smaller than for the scheme with optical isolation between the Cr^{2+}:ZnSe and Tm:YLF lasers [25].

4. Tuning of the Cr^{2+}:ZnSe laser wavelength in the range 2.53–2.75 μm

To obtain lasing in the Cr^{2+}:ZnSe polycrystal in the long-wavelength region of its gain spectrum, we used mirrors that ensured a high Q-factor of the cavity at $\lambda = 2.6–3.0$ μm. These mirrors allowed us to realise a simple scheme of a two-mirror linear cavity (without an intermediate dichroic deflecting mirror). Pumping occurred through a dichroic highly reflecting mirror with a transmission coefficient of ~80% at the pump wavelength. The output mirror had a transmission coefficient of 20%–25% at $\lambda = 2.6–3.0$ μm. Both mirrors were transparent in the short-wavelength region ($\lambda < 2.55$ μm).

Tuning was performed in the range $\Delta\lambda \approx 2530–2750$ nm (Fig. 8). Despite the fact that the selective polarisation losses were decreased due to the absence of the intermediate deflecting mirror, the laser spectrum showed no background radiation outside the maximum of the filter transmission.

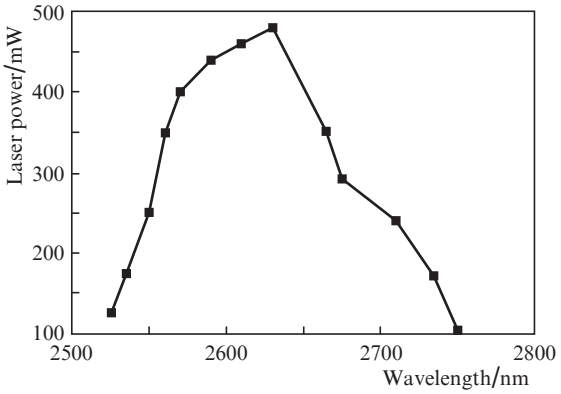

Figure 8. Tuning curve of the Cr^{2+}:ZnSe laser in the long-wavelength region at a pump power of 1.8 W.

The laser output power was ~2 W (λ = 2.6 μm) at a pump power of 6 W. The maximum slope efficiency was 50% at the linear part of the dependence of the laser power on the pump power, while the efficiency with respect to the absorbed power was ~67% taking into account the losses at the dichroic mirror (absorption of pump power in the crystal ~70%).

5. Conclusions

Thus, we experimentally studied the spectral and lasing characteristics of a repetitively pulsed laser based on a Cr^{2+}:ZnSe polycrystal with a selective cavity.

A method of determining the selective characteristics of a dispersive cavity with a prism is described.

It is found that, for polarisation isolation of the plates of the Lyot filter at the laser pulse duration $\Delta t_{gen} \approx 70$ ns, it is necessary to use additional partial polarisers.

The laser wavelength was tuned within the ranges 2.07–2.4 μm and 2.53–2.75 μm. The narrowest linewidth was $\delta\lambda \approx 4$ nm.

The maximum slope efficiency was ~50% at the laser wavelength λ = 2.6 μm.

The obtained results can be used for development of tunable Cr^{2+}:ZnSe lasers with required spectral characteristics.

Acknowledgements. The authors thank E.M. Gavrishchuk and S.S. Balabanov (Institute of Chemistry of High-Purity Substances, Russian Academy of Sciences) for providing Cr^{2+}:ZnSe samples. This work was supported by the Analytical Departmental Targeted Program 'Development of the Scientific Potential of the Higher School' (Project No. 2.1.1/3603) and by the Federal Targeted Program 'Scientists and Science Educators of Innovative Russia' (Contract No. 02.740.11.0563).

References

1. Godard A. *C.R. Phys.*, **8**, 1100 (2007).
2. Akimov V.A., Kozlovskii V.I., Korostelin Yu.V., Landman A.I., et al. *Kvantovaya Elektron.*, **34** (2), 185 (2004) [*Quantum Electron.*, **34** (2), 185 (2004)].
3. Akimov V.A., Kozlovskii V.I., Korostelin Yu.V., Landman A.I., et al. *Kvantovaya Elektron.*, **35** (5), 425 (2005) [*Quantum Electron.*, **35** (5), 425 (2005)].
4. Sorokin E., Sorokina I.T., Fisher C., Sigrist M.W. *Proc. Conf. on Advanced Solid-State Photonics* (Vienna, Austria, 2005) paper MD4.
5. Bernhardt B., Sorokin E., Jacquet P., Thon R., Becker T., Sorokina I.T., Picqué N., Hänsch T.W. *Appl. Phys. B*, **100**, 3 (2010).
6. Zakharov N.G., Savikin A.P., Sharkov V.V., Eremeikin O.N. *Opt. Spektrosk.*, **112**, 35 (2012).
7. Wagner G., Carrig T., Page R., Schaffers K., Ndap J., Ma X., Burger A. *Opt. Lett.*, **24**, 19 (1999).
8. Graham K., Fedorov V.V, Mirov S.B, Doroshenko M.E., Basiev T.T., Orlovskii Yu.V., et al. *Kvantovaya Elektron.*, **34** (1), 8 (2004) [*Quantum Electron.*, **34** (1), 8 (2004)].
9. Sennaroglu A., Demirbas U., Vermeulen N., Ottevaere H., Thienpont H. *Opt. Commun.*, **268**, 115 (2006).
10. Demirbas U., Sennaroglu A. *Opt. Lett.*, **31**, 2293 (2006).
11. Doroshenko M., Koranda P., Jelínková H., Šulc J., Basiev T.T., Komar V.K., Kosmyna M. *Proc. SPIE Int. Soc. Opt. Eng.*, **6190**, 61901F (2006).
12. Doroshenko M.E., Jelínková H., Koranda P., Šulc J., Basiev T.T., Osiko V.V., Komar V.K., et al. *Laser Phys. Lett.*, **7**, 38 (2010).
13. Sorokin E., Sorokina I.T., Mirov M.S., Fedorov V.V., Moskalev I.S., Mirov S.B. *Proc. Conf. on Advanced Solid-State Photonics* (San Diego, USA, 2010) paper AMC2.
14. Sorokina I.T., Sorokin E., Di Lieto A., Tonelli M., Page R.H., Schaffers K.I. *J. Opt. Soc. Am. B*, **18**, 926 (2001).
15. Koranda P., Šulc J., Doroshenko M., Jelínková H., Basiev T.T., Osiko V., et al. *Proc. SPIE Int. Soc. Opt. Eng.*, **7578**, 757826 (2010).
16. Moskalev I.S., Fedorov V.V., Mirov S.B. *Opt. Express*, **16**, 4145 (2008).
17. Moskalev I.S., Fedorov V.V., Mirov S.B. *Proc. Conf. on Advanced Solid-State Photonics* (San Diego, USA, 2010) paper ATuA11.
18. Berry P.A., Schepler K.L. *Opt. Express*, **18**, 15062 (2010).
19. Zaidel' A.N., Ostrovskaya G.V., Ostrovskii Yu.I. *Tekhnika i practika spektroskopii* (Technique and Practice of Spectroscopy) (Moscow: Nauka, 1972).
20. Anokhov S.P., Marusii T.Ya., Soskin M.S. *Perestraivaemye Lasery* (Tunable Lasers) (Moscow: Radio i Svyaz', 1989).
21. Bloom A.L. *J. Opt. Soc. Am.*, **64**, 447 (1974).
22. Hodgkinson I.J., Vukusic J.I. *Appl. Opt.*, **17**, 1944 (1978).
23. Zhu S. *Appl. Opt.*, **29**, 410 (1990).
24. Gurzadyan G.G., Dmitriev V.G., Nikogosyan D.N. *Nelineino-opticheskie kristally. Svoistva i primenenie v kvantovoi electronike. Spravochnik* (Nonlinear Optical Crystals. Properties and Application in Quantum Electronics. Handbook) (Moscow: Radio i Svyaz', 1991).
25. Vladykin A.V., Eremeikin O.N., Zakharov N.G., et al. *Vestnik NNGU. Ser. Optika i Kvant. Elektron.*, **5**, 79 (2011).